*Materials Science-Poland, Vol. 23, No. 3, 2005*

# Multilayer $Al_2O_3$/Mo composites

H. MATYSIAK[1*], Ł. CIUPIŃSKI[2], A. OLSZYNA[1], K. J. KURZYDŁOWSKI[1]

[1]Faculty of Materials Science and Engineering, Warsaw University of Technology, ul. Wołoska 141, 02-507 Warsaw, Poland

[2]Functional Materials Research Center, Warsaw University of Technology, ul. Wołoska 141, 02-507 Warsaw, Poland

The present study was concerned with multilayer composites of the .../$Al_2O_3$/$Al_2O_3$ + *x* vol. % Mo/$Al_2O_3$ type produced by tape casting. Molybdenum content in individual layers of the composites varied from 4 to 28 vol. %. The densities, porosities, Young moduli, bending strengths, and fracture toughnessess of the composites were measured. The residual stress in the layers was analysed by FEM. Investigations of the composite microstructures revealed: $\alpha$-$Al_2O_3$, Mo, and $Mo_2C$. After sintering, the composites had a high relative density (the porosity $P_c$ did not exceed 10%). As the volumetric content of molybdenum increased, the densities of the composites increased, whereas their Young moduli $E$ decreased. The highest values of the bending strength $\sigma_b$ (819 MPa), stress intensity factor $K_{IC}$ (7.75MPa·m$^{1/2}$), and cracking energy $\gamma$ (102 J/m$^2$) were obtained in the composite with the 14 vol. % molybdenum content. The strength $\sigma_b$ and fracture toughness of this composite were more than two times higher than those of $Al_2O_3$, and the cracking energy – six times. These values can be partly explained in terms of the compressive residual stress in the composite layers.

Key words: *tape casting; fracture toughness; residual stress*

## 1. Introduction

Multilayer composites are materials composed of a number of layers with properties varying from one layer to another in a way depending on their phase composition. In current practice, the component layers can be ceramic, metallic or polymeric, and their thickness may range from nanometers to millimetres [1]. Multi-layered composites are produced using various techniques, such as CVD, PVD, plasma spraying, electrophoresis, powder sintering, and tape casting. They exhibit increased mechanical strength and strain to failure, as well as improved fracture toughness. This is in general due to the interactions of the crack with the transition layers and residual stress fields existing within the material. More specifically, the following mechanisms

* Corresponding author, e-mail: huba@inmat.pw.edu.pl

have been identified to contribute to the increased fracture toughness of multilayer composites [2–23]:

- crack deflection due to lower cracking energy, lower strength, or a decreased rigidity in composites – a weak layer or a weak interlayer,
- crack deflection due to compressive or tensile residual stresses in the individual layers of the composite,
- phase transformation hardening, occurring in composites that, in layers of a certain type, contain a metastable form of zirconium oxide,
- crack bridging mechanisms, occurring in ceramic/metal composites.

From the above discussion, it can be concluded that residual stress is one of the important factors influencing the strength of multi-layered composites. Residual stress in metal-ceramic composites is of technological origin. The sintering process, which is a common technique used for the fabrication of multilayer ceramic composites, may be divided into three basic steps: heating, annealing, and cooling. Annealing generates stresses in the composite layers, because of the differences in the sintering kinetics of the individual components. These stresses can result in the material cracking at high temperatures or induce preferred centres of crack initiation during the cooling operation. During the cooling stage, residual stresses are generated due to differences in the linear thermal expansion coefficient $\alpha$ between components.

The increase of fracture toughness due to residual stress is principally related to the crack deflection effect. Developing cracks deflect from their energetically preferred propagation direction by compressive stress in the microstructure. This mechanism increases the effective crack path and cracking energy, thereby increasing the fracture toughness of the composite [8–10, 14–21]. Its relevance obviously depends on the value and spatial distribution of residual compressive stresses.

The aim of the study was to develop multiplayer $Al_2O_3$/Mo composites with increased fracture toughness. Moreover, the selected composite production technique was tape casting, which is relatively inexpensive and can be used to fabricate large components. The technological routes used here allow the production of ceramic/metal composites with volume fractions of the metal ranging from 4 to 28% of the volume, without visible sedimentation of Mo particles in spite of the large difference in the densities of the components.

## 2. Experimental

The composites were produced using AKP-50 $\alpha$-$Al_2O_3$ powder from Sumitomo Chemical Co. Ltd., and MO006020 Mo powder from Goodfellow Advanced Materials. Test specimens were prepared by the tape casting method [27]. The procedure used here consisted of the following steps:

- Preparation of the cast composition containing the powder ($Al_2O_3$ or $Al_2O_3$ + $x$ % Mo), binder (PVB resin), softener (dibutyl phthalate), solvent (ethanol and TRI), and flux (linseed oil) via mixing in a RETSCH agate mill for $t$ = 4 h.

• Casting of a foil, which was subsequently dried and cut according to the assumed shape of specimens. The as-cast foil thickness was $g$ = 1 mm and the casting rate $V$ = 0.5 m/min. The foil was dried at room temperature.

• Arranging the foils in packets in a die and subsequent lamination under uniaxial pressing using a TM4 hydraulic press ($p$ = 10 MPa).

• Isostatic consolidation in an autoclave under pressure ($p$ = 120 MPa).

• Sintering in a Lenton-Thermal furnace at $T$ = 1473 K in an $N_2$ atmosphere for $t$ = 1 h (a), in a Baltzers furnace in vacuum ($p = 10^{-4}$ Pa) at $T$ = 1973 K for $t$ = 1.5 h (b).

The densities and porosities of the specimens were determined by the Archimedes method using a Radwag WPS balance. The qualitative characterisation of the microstructures was based on light microscopy images (Nikon Epiphot) at magnifications ranging from 100 to 1000×. The Young moduli ($E$) were determined by the ultrasonic method using an UR19A refractometer. The bending strengths of the composites were measured with an Instron 1114 strength machine in the three-point bending mode using 6×4×50 mm bars (10 samples from each type of composite). The support spacing used was $L$ = 40 mm. Specimens were loaded at a rate of 1 mm/min until failure, and the failure force was measured. A similar three-point bending setup was used to determine the stress intensity factors. Test specimens (8 bars 6×4×50 mm from each type of composite) were notched, in their mid-length, to a depth of $a$ = 1.1 mm. The notching was made stepwise, using a 0.2 mm diamond saw down to a depth of 0.9 mm and then a 0.025 mm diamond saw. The support spacing used this time was $L$ = 15 mm.

The cracking energy was calculated from the relationship $\gamma = K_{IC}^2/2E$, where $K_{IC}$ is the stress intensity factor. The distribution and magnitude of the residual stress occurring in the composites as a result of cooling were modelled using Ansys 5.7 software. For the purpose of modelling, a representative volume was selected in the way schematically shown in Fig. 1. The modelled representative composite volume contained 2 complete and 2 halves of composite layers. An initial thickness of the layers of 1 mm was assumed, which corresponds to the thickness of the as-cast foil.

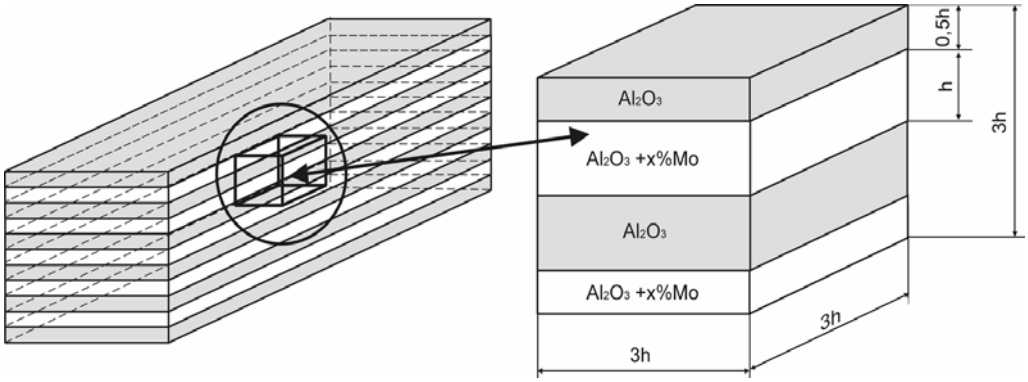


Fig. 1. Geometrical model of the layered composite structure adopted in the FEM analysis of residual stress

In the analysis, the materials of the individual layers ($\alpha$-$Al_2O_3$ layers and the $Al_2O_3$ + $x$ % Mo composite layers) were modelled as perfectly elastic. In this case, their macroscopic behaviours can be described by the Young moduli $E$ and Poisson ratios. The Young moduli of alumina and Mo as a function of temperature are shown in Fig. 2a. Additionally, the Poisson ratio for corundum was assumed to be invariant with temperature and equal to 0.23. Variations of $\alpha$ for alumina and molybdenum are shown in Fig. 2b.

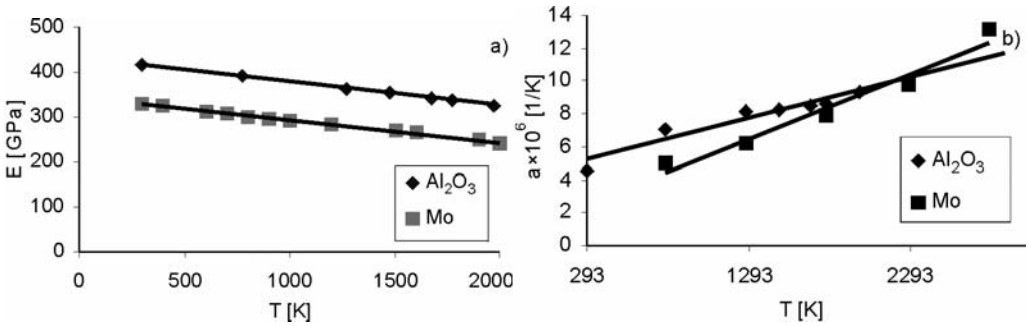


Fig. 2. The variations of the Young moduli (a) and linear thermal expansion coefficients $\alpha$ (b) in corundum and molybdenum as functions of temperature [25, 26]

For the generation of the FE mesh, a 20 nodes "cubic" structural element (Solid 95) was employed. Figure 3 shows the assumed geometry of the model and the mesh of finite elements. The straight line $P$ shown in the figure denotes the path along which the stress distributions were analysed.

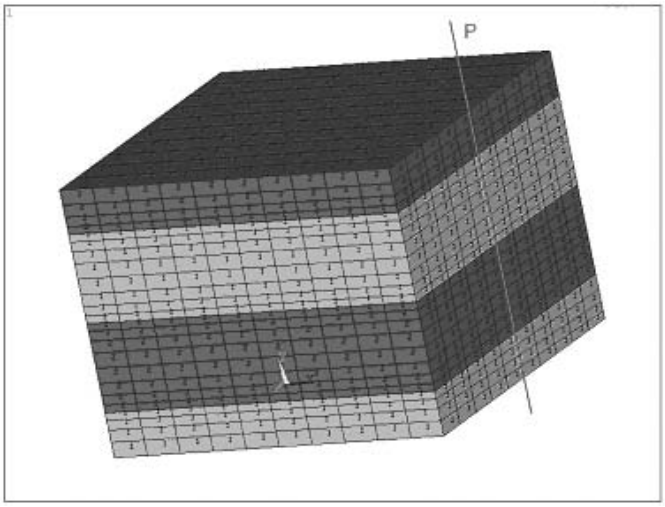


Fig. 3. Geometry of the model and the mesh of finite elements. Line $P$ shown in the figure denotes the path along which the stress distributions were analysed

Two different boundary conditions were assumed in the modelling:

**Model 1:**

- symmetric with respect to the planes $\{X,Y,Z\} = 0$,
- the displacements $u_x$, $u_y$, and $u_z$ of the nodes positioned in the planes $X = 3h$, $Y = 3h$, and $Z = 3h$, respectively, along the respective directions normal to these planes, are coupled.

**Model 2:**

- symmetric with respect to the planes $\{X,Y,Z\} = 0$,
- only the displacements $u_x$ and $u_y$ of the nodes positioned in the planes $X = 3h$ and $Y = 3h$, respectively, along the directions normal to these plane, are coupled.

It was assumed that the internal stress is generated when the composites are cooled from the sintering temperature $T_S$ (1973 K) to room temperature $T_r$ (293 K), as a result of differences in the linear expansion coefficients $\alpha$ of their components. Accordingly, as the load imposed on the models, a temperature drop of 1680 K was used. Figure 2b shows the values of the linear expansion coefficients of the individual components of the layered composites. Since no experimental data were available as to the coefficient $\alpha$ for $Al_2O_3$ + *x* % Mo composite layers, these values were calculated based on the rule of mixtures.

## 3. Results and discussion

Figures 4a–e show examples of the structures of the examined multilayer composites. Microscopic observations revealed that the molybdenum particles were uniformly distributed throughout the volumes of the composites. In the composites with molybdenum content up to 14 vol. %, the individual layers and the interlayer boundaries did not contain defects generated during the fabrication process, whereas in specimens with 21 and 28 vol. % of molybdenum, the composite microstructures contained numerous cracks formed during fabrication. These cracks developed in the $Al_2O_3$ layers, but no transverse cracks were observed within the composite layers. There were also delaminating cracks, which propagated along interlayer boundaries.

Table 1 lists selected properties of the fabricated multilayer $Al_2O_3$/Mo composites. The sintered composites had a fairly good relative density (the porosity $P_c$ did not exceed 10%). With increasing volumetric content of molybdenum, the density d increases linearly, whereas the Young modulus $E$ decreases in similar way. This suggests that the studied structure can be assumed to vary primarily in the content of Mo. The highest values of the bending strength $\sigma_b$ (819MPa), the stress intensity factor $K_{IC}$ (7.75 MPa·m$^{1/2}$), and the cracking energy $\gamma$ (102 J/m$^2$) were observed in the composite with 14 vol. % of molybdenum in the individual layers. The mechanical strength $\sigma_b$ and fracture toughness of this composite are more than twice higher than for $Al_2O_3$, and the cracking energy more than 6 times higher.

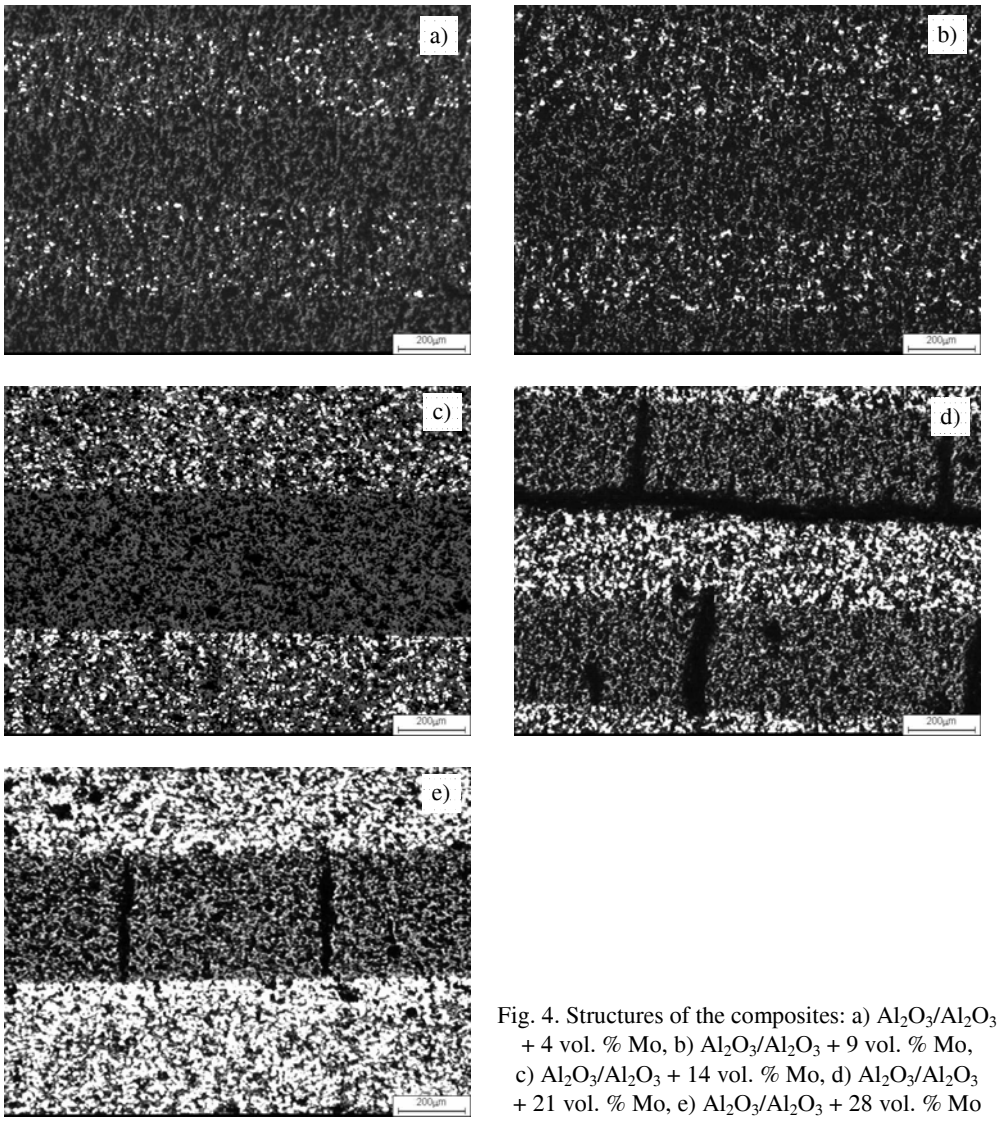


Fig. 4. Structures of the composites: a) $Al_2O_3/Al_2O_3$ + 4 vol. % Mo, b) $Al_2O_3/Al_2O_3$ + 9 vol. % Mo, c) $Al_2O_3/Al_2O_3$ + 14 vol. % Mo, d) $Al_2O_3/Al_2O_3$ + 21 vol. % Mo, e) $Al_2O_3/Al_2O_3$ + 28 vol. % Mo

Table 1. Mechanical properties (density $d$, porosity $P_c$, Young modulus $E$, bending strength $\sigma_b$, fracture toughness $K_{IC}$, cracking energy $\gamma$) of the $Al_2O_3/Al_2O_3$ + $x$ vol. % Mo composites

| $x$ % vol. Mo | $d$ [g/cm$^3$] | $P_c$ [%] | $E$ [GPa] | $\sigma_b$ [MPa] | $K_{IC}$ [MPa·m$^{1/2}$] | $\gamma$ [J/m$^2$] |
|---|---|---|---|---|---|---|
| 0 | 3.98 | 0 | 400 | 380 | 3.5 | 15 |
| 4 | 3.86 | 6 | 336±14 | 420±80 | 4.7±0.4 | 33±5 |
| 9 | 3.85 | 10 | 313±4 | 590±70 | 6.0±0.7 | 59±14 |
| 14 | 4.22 | 4 | 297±4 | 820±30 | 7.8±0.66 | 102±15 |
| 21 | 4.39 | 4 | 287±8 | 560±50 | 6.5±0.9 | 74±19 |
| 28 | 4.59 | 3 | 276±7 | 350±30 | 6.0±0.7 | 67±16 |

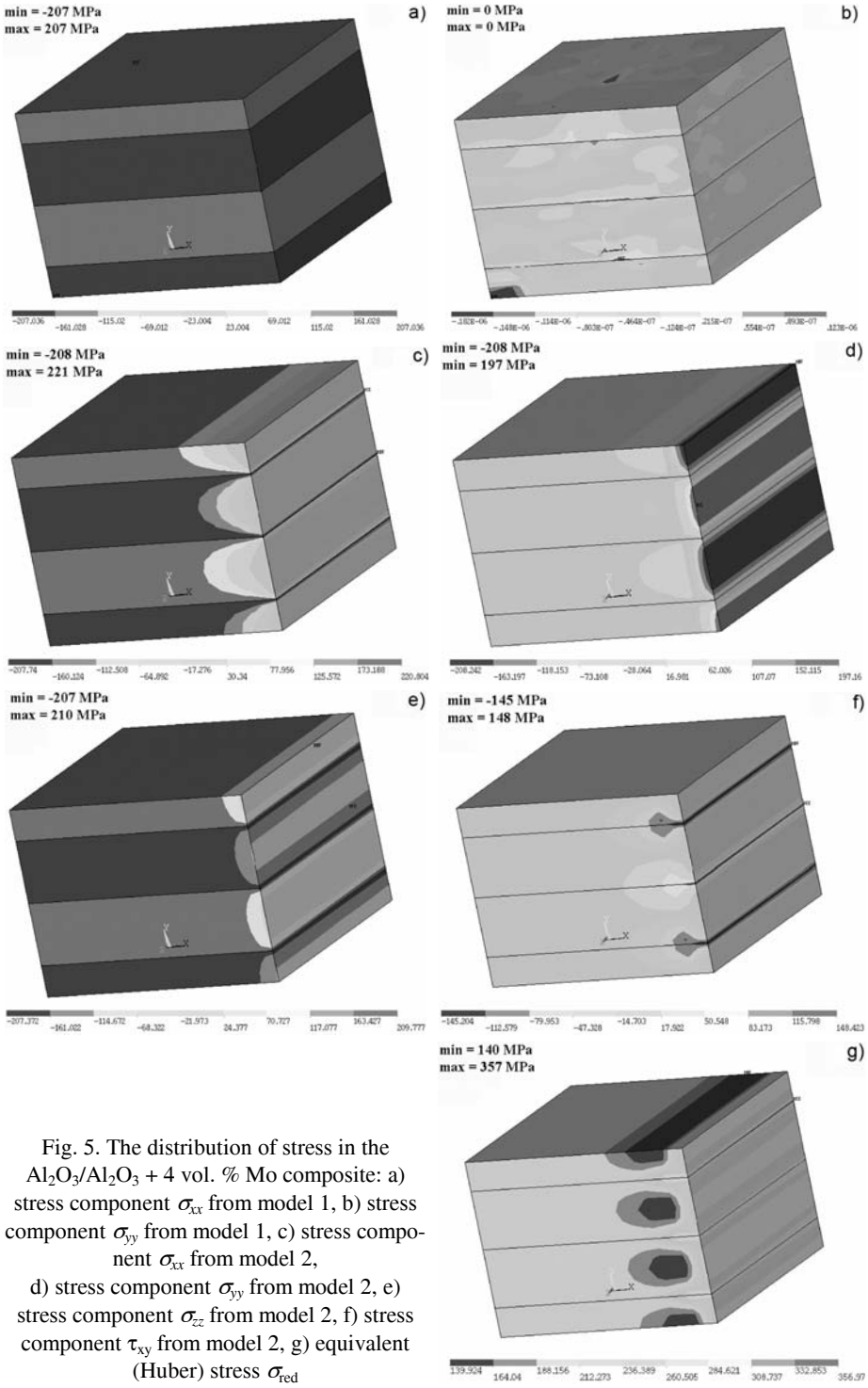


Fig. 5. The distribution of stress in the $Al_2O_3/Al_2O_3$ + 4 vol. % Mo composite: a) stress component $\sigma_{xx}$ from model 1, b) stress component $\sigma_{yy}$ from model 1, c) stress component $\sigma_{xx}$ from model 2, d) stress component $\sigma_{yy}$ from model 2, e) stress component $\sigma_{zz}$ from model 2, f) stress component $\tau_{xy}$ from model 2, g) equivalent (Huber) stress $\sigma_{red}$

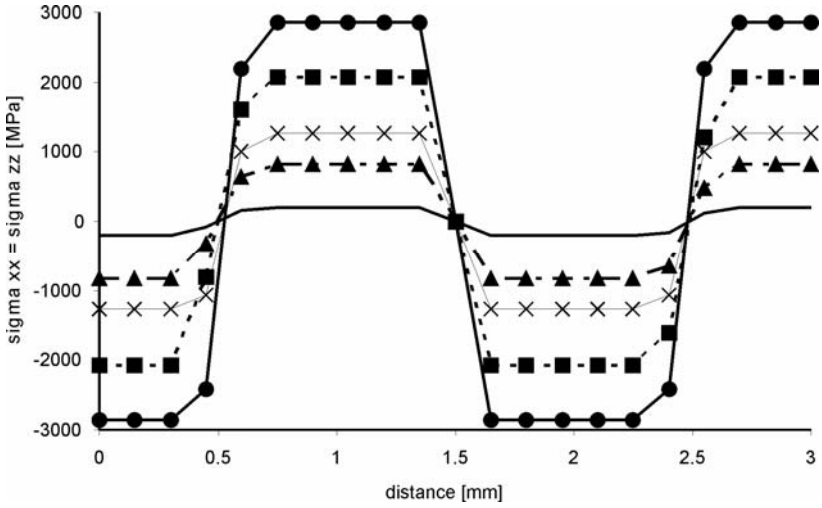


Fig. 6. Variation of the residual stress tensor component $\sigma_{xx} = \sigma_{zz}$ as a function of the distance along the line $P$ in multilayer $Al_2O_3/Al_2O_3 + x$ vol. % Mo composites (Model 2): ▬ – $x = 4$, ▲ – $x = 9$, × – $x = 14$, ■ – $x = 21$, ● – $x = 28$

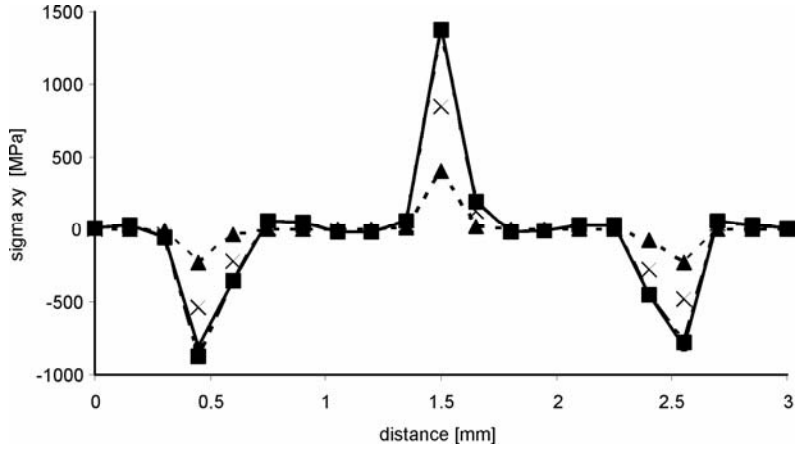


Fig. 7. Variations of the components $\sigma_{xy}$, $\sigma_{xz}$, and $\sigma_{yz}$ of the residual stress tensor as a function of the distance along the line $P$ in multi-layer $Al_2O_3/Al_2O_3 + x$ vol. % Mo composites: ▬ – $x = 4$, ▲ – $x = 9$, × – $x = 14$, ■ – $x = 21$

Figures 5–7 show the results of the analysis of residual stresses, performed using the Finite Elements Method. Since the characters of the stress distributions are identical for all the analysed models of the composite structures, only the results obtained for the $Al_2O_3/Al_2O_3$ + 4 vol. % Mo composite are shown. The description given is based on the numerical results of all modelled cases.

**Model 1.** The distributions and values of the stress tensor components $\sigma_{xx}$ and $\sigma_{zz}$ (the stresses whose mutually perpendicular directions lie in the plane of the interlayer

boundary) are identical. In $Al_2O_3$ layers, these stress components are tensile, whereas in $Al_2O_3$ + $x$ vol. % Mo composite layers they are compressive. The magnitudes of these stresses increase with increasing molybdenum content in the layers. At the interlayer boundary, the magnitude of stress abruptly changes in a step-wise manner. The stress component $\sigma_{yy}$ (acting in the direction perpendicular to the interlayer boundary plane) is zero, irrespective of the molybdenum content in the composite layer.

**Model 2.** The effect of a free surface due to the removal of the condition on the displacements $u_z$ of the nodes positioned in the plane $Z = 3h$ essentially changes the distributions of stress tensor components. The components $\sigma_{xx}$ and $\sigma_{zz}$ are equal to zero, and, as the distance from this surface towards the interior of the material increases, the stress magnitudes increase and reach their maximum values (tension in the $Al_2O_3$ layers and compression in the composite layer) equal to those adopted in model 2. It should be noted, however, that in the immediate vicinity of the entire interlayer boundary the components $\sigma_{xx}$ and $\sigma_{zz}$ reach their maximum values. The stress $\sigma_{yy}$, on the other hand, reaches its maximum value in the plane of the free surface and then decreases to zero in the interior just as is the case of model 2.

Another consequence of the presence of the free surface is the shear stress $\sigma_{xy}$ ($\sigma_{xz}$ and $\sigma_{yz}$ are zero). The largest stress $\sigma_{xy}$ is generated at the interlayer boundary. In terms of the von Mises–Huber criterion, the most stressed components of multilayer composites are the interlayer boundaries.

The geometry of the composite structure model considered here appears to be sufficient for an analysis of the residual stress. The character of the distributions of stress tensor components obtained from this analysis are consistent with the qualitative analysis of the material properties of the composite constituents.

The calculated average values considerably exceed the tensile strength of alumina (except in the composite with the lowest molybdenum content). The transverse and delaminating cracks in $Al_2O_3$ layers, however, are observed only in composites with 21 and 28 vol. % molybdenum content.

This can be attributed to the assumption that the $Al_2O_3$ + $x$ vol. % Mo composite layers are uniform and purely elastic in the early stages of sintering. On the other hand, the stress distributions calculated here give better insight into the mechanics of multi-layered composites.

## 4. Conclusions

The tape casting technique used in the present experiment permitted the fabrication of ceramic/metal composites with a wide range of metal volumetric content (4 to 28 vol. % Mo) and porosity (1 to 10%). The densities of the composites did not exceed 5.5 g/cm$^3$, i.e. 138% of the density of alumina.

The best properties were obtained for the composite with 14 vol. % of Mo. The fracture toughness of this composite was twice that of $Al_2O_3$. This was accompanied by a six-fold increase of the cracking energy and bending strength.

The proposed FEM model of two-fold layered composites is useful for the qualitative analysis of residual stress arising during cooling from the fabrication temperature. Quantitative analyses of stress require that it be modified to take into account the visco-elastic behaviour during the early stages of cooling.

**Aknowledgements**

This work was supported by the State Committee for Scientific Research (grant No. 4T08D00223).

## References

[1] CAHN R.W., HAASEN P., KRAMER E.J., *Materials Science and Technology. Structure and Properties of Ceramics*, Vol. 11, CH, Weinheim, 1994.
[2] MARSHALL D.B., RATTO J.J., LANG F.F., J. Am. Cer. Soc., 74 (1991), 2979.
[3] KOVAR D., THOULESS M.D., HALLORAN J.W., J. Am. Cer. Soc., 81 (1998), 1004.
[4] HUANG Y., CAI S., GUO H., WANG C., XIE Z., *The Biomimetric Structure Design and Preparation of $Si_3N_4$ Matrix Composites with High Toughness*, 9th Cimtec-World Ceramics Congress 2000, pp. 881–888.
[5] ZENG Y., JIANG D., Fabrication and properties of laminated $Al_2O_3$/TiC composites, Cer. Int., 27 (2002), 597.
[6] MING L.Y., WEI P., SHUGIN L., JIAN CH., RUIGANG W., JIANQUING LI, Cer. Int., 28 (2002), 223.
[7] DREWNY E.N., MOON R.J., BOWMAN K.J., TRUMBLE K.P., BREMM J., Scripta Materialia, 41 (1999), 749.
[8] CAI P.Z., GREEN D.J., MESSING G.L., J. Am. Cer. Soc., 80 (1997), 1929.
[9] CAI P.Z., GREEN D.J., MESSING G.L., J. Am. Cer. Soc., 80 (1997), 1940.
[10] GREEN D.J., CAI P.Z., MESSING G.L., J. European Cer. Soc., 19 (1999), 2511.
[11] FOLSOM C.A., ZOK F.W., LANGE F.F., J. Am. Cer. Soc., 77 (1994), 689.
[12] OECHSNER M., HILLMAN C., LANGE F.F., J. Am. Cer. Soc., 79 (1996), 1834.
[13] WANG H., XIAOZHI H., J. Am. Cer. Soc., 79 (1994), 553.
[14] SERGO V., LIPKIN D.M., DE PORTU G., CLARKE D.R., J. Am. Cer. Soc., 80 (1997), 1633.
[15] LAKSHMINARAYANAN R., SHETTY D.K., CUTLER R.A., J. Am. Cer. Soc., 79 (1996), 79.
[16] MARSHALL D.B., MORGAN P.E.D., HOUSLEY R.M., J. Am. Cer. Soc., 80 (1997), 1677.
[17] CUTLER W.A., ZOK F.W., LANGE F.F., J. Am. Cer. Soc., 80, (1997), 3029.
[18] MOON R.J., BOWMAN K.J., TRUMBLE K.P., RODEL J., Acta Mater., 49 (2001), 995.
[19] LUCCHINI E., SBAIZERO O., J. European Cer. Soc., 15 (1995), 975.
[20] CAI P.Z., GREEN D.J., MESSING G.L., J. European Cer. Soc., 5 (1998), 2025.
[21] ZHANG G-J., YUE X-M., WATANABE T., J. European Cer. Soc., 19 (1999), 2111.
[22] JIMENEZ-MELENDO M., GUTIERERREZ-MORA F., DOMINGUEZ-RODRIGUEZ A., Acta Mater., 48 (2000), 4715.
[23] HWU K.L., DERBY B., Acta Mater., 47 (1999), 545.
[24] CHENG Z., MECHOLSKY J.J., J. Am. Cer. Soc., 76 (1993), 1258.
[25] http://michelle.ucsd.edu/lib/props/panos/moa.html.
[26] MUNRO R.G., J. Am. Cer. Soc., 80 (1997), 1919.
[27] MISTLER R.E., TWINAME E.R., *Tape Casting: Theory and Practice*, American Ceramic Society, Westerville, OH, 2000.

*Received 3 December 2004*
*Revised 5 August 2005*